Spa32 interaction with the inner-membrane Spa40 component of the type III secretion system of Shigella flexneri is required for the control of the needle length by a molecular tape measure mechanism

Botteaux, Anne; Sani, Musa; Kayath, Christian A.; Boekema, Egbert J.; Allaoui, Abdelmounaaim; Allaoui, Abdelmounaaïm

Published in:
Molecular Microbiology

DOI:
10.1111/j.1365-2958.2008.06499.x

Publication date:
2008

Molecular Microbiology (2008) 70(6), 1515–1528 ■
doi:10.1111/j.1365-2958.2008.06499.x
First published online 31 October 2008

Spa32 interaction with the inner-membrane Spa40 component of the type III secretion system of *Shigella flexneri* is required for the control of the needle length by a molecular tape measure mechanism

Anne Botteaux,[1‡] Musa Sani,[2†‡] Christian A. Kayath,[1‡] Egbert J. Boekema[2] and Abdelmounaaïm Allaoui[1*]
[1]*Laboratoire de Bactériologie Moléculaire, Faculté de Médecine, Université Libre de Bruxelles (ULB), Route de Lennik, 808, 1070, Bruxelles, Belgium.*
[2]*Biophysical Chemistry, Groningen Biomolecular Sciences and Biotechnology Institute, University of Groningen, Groningen, The Netherlands.*

Summary

The effectors of enterocyte invasion by *Shigella* are dependent on a type III secretion system that contains a needle whose length average does not exceed 50 nm. Previously, we reported that Spa32 is required for needle length control as well as to switch substrate specificity from MxiH to Ipa proteins secretion. To identify functional domains of Spa32, 11 truncated variants were constructed and analysed for their capacity (i) to control the needle's length; (ii) to secrete the Ipa proteins; and (iii) to invade HeLa cells. Deletion at either the N-terminus or C-terminus affect Spa32 function in all cases, but Spa32 variants lacking internal residues 37–94 or 130–159 retained full Spa32 function. Similarly, a Spa32 variant obtained by inserting of the YscP's ruler domain retained Spa32 function although it programmed slightly elongated needles. Using the GST pull-down assay, we show that residues 206–246 are required for Spa32 binding to the C-terminus of Spa40, an inner membrane protein required for Ipa proteins secretion. Our data clearly demonstrate that shortening Spa32 affects the length of the needle in a comparable manner to the *spa32* mutant, indicating that the control of needle length does not require a molecular ruler mechanism.

Accepted 8 October, 2008. *For correspondence. E-mail aallaoui@ulb.ac.be; Tel. (+32) 2 5556251; Fax (+32) 2 5556116. †Present address: Division of Tumour Biology, the Netherlands Cancer Institute-Antoni van Leeuwenhoek Hospital, Plesmanlaan 121, 1066 CX, Amsterdam, The Netherlands. ‡These authors contributed equally to this work.

Introduction

Shigella flexneri is the aetiological agent of the endemic form of bacillary dysentery. This Gram-negative bacterium causes disease by invading the colonic mucosa (Hale, 1991). The pathogenesis of *Shigella* is attributed to the organism's ability to invade, replicate and spread intercellularly within the colonic epithelium. The invasion of host cells by *Shigella* spp. is a complex multifactorial event that involves many different bacterial proteins. Many of the genes for key *Shigella* virulence proteins are located on a 214 kb plasmid and are conserved in all *Shigella* spp. All bacterial genes necessary for entry into host cells have been identified (Parsot *et al*., 2005). They are clustered within a 30 kb region of a large virulence plasmid. This region carries two types of genes: the *ipa* and *ipg* encoding the entry-mediating proteins and their individual intrabacterial chaperones (Parsot *et al*., 2005; Espina *et al*., 2006; Sani *et al*., 2007a), and the *mxi* and *spa* genes that code for proteins forming a type III secretion system (T3SS) (Blocker *et al*., 2001). This system is found in many other pathogenic Gram-negative bacterial species that have developed diverse survival strategies within their hosts (Hueck, 1998). Upon contact with host cells, a major function of the T3SS is to transport proteins from the bacterial cytoplasm either into the cytosol or to the cytosolic face of the membrane (Cornelis, 2006). Kubori *et al*. (1998) and Blocker *et al*. (1999; 2001) identified and biochemically isolated the macromolecular structure formed by the *Salmonella* and *Shigella* type III secretons. They described this organelle as a cylindrically symmetrical object composed of two parts: a 7–8 nm wide and 50 nm long needle emanating from the bacterial surface and a shorter cylinder, formed by a succession of plates (20–40 nm in diameter) presumed to span the inner and outer bacterial membranes and the peptidoglycan. Analysis of electron microscopy (EM) images of the 'needle complex' (NC) from *Shigella* indicated that the needle and

base contain a central 2–3 nm canal (Blocker *et al*., 2001; Sani *et al*., 2007b). Six major NC components, MxiD, MxiG, MxiJ, MxiH, MxiI and MxiM (Blocker *et al*., 2001; Sani *et al*., 2007b), have so far been identified to form the NC.

One of the remarkable features of all described type III secretion apparatus (T3SA) is that the length of the needle, a hollow tubular structure, is fairly well controlled at approximately 50 nm in *Shigella*, 60 nm in *Yersinia enterocolitica* and 55 nm in the SPI1-encoded T3SA of *Salmonella* (Blocker *et al*., 1999; Kimbrough and Miller, 2000; Kubori *et al*., 2000; Journet *et al*., 2003). Similarly, the hook length in the flagellar structure is also controlled at around 55 nm in wild-type *Salmonella* (Hirano *et al*., 1994). The length of the T3SS needle was genetically investigated by mutations in *spa32* from *Shigella* (Magdalena *et al*., 2002; Tamano *et al*., 2002), in *invJ* from *Salmonella* (SPI1) (Kubori *et al*., 2000) and in *yscP* from *Y. enterocolitica* (Journet *et al*., 2003). The length of the flagellum hook was also investigated by mutation in *fliK* from *Salmonella* (Williams *et al*., 1996). All mutants exhibit abnormal long needles or hooks that are up to 20 times longer than those observed in wild-type strains. In addition, *invJ*, *yscP* and *spa32* mutants are unable to secrete the Sip, Yop or Ipa substrates respectively (Kubori *et al*., 2000; Magdalena *et al*., 2002; Journet *et al*., 2003).

At least three models were proposed to explain how the needle/hook length is controlled (Minamino and Pugsley, 2005; Marlovits *et al*., 2006). The first one is related to *Salmonella* flagellar hook length control. FliK, believed to be the hook length sensor, interacts with FlhB, an integral membrane export apparatus component, to change its export specificity upon hook completion at approximately 55 nm in wild-type flagella. Makishima *et al*. (2001) proposed the measuring-cup model in which the hook length is determined by the capacity of the C-ring, which somehow measures the exported amount of FlgE, the hook component. The second major length control model comes from the study of YscP of *Yersinia*, which determines the length of the needle protein YscF by acting as a molecular ruler (Journet *et al*., 2003). The length of the *Yersinia* injectisome is controlled by *yscP*, a homologue of *fliK* (Journet *et al*., 2003). Indeed, lengthening or shortening the central part of YscP by amino-acid insertion or deletion causes concomitant changes in needle length (Journet *et al*., 2003; Cornelis, 2006). More recently, Moriya *et al*. (2006) suggested that FliK acts as a flexible tape measure, but that hook length is also dependent on the hook elongation rate and a switch timing mechanism. In this model, the size of the hook structure depends on the rate of hook polymerization (governed by FlgE concentration) and the frequency of FliK export (in turn, governed by the interaction rate of FliK with FlgE and FlgD). The diameter of the central channel of the flagellum is only 2 nm, so according to this model FliK must be in an extended conformation in the central channel and functions as a hook-length controller only during its infrequent export process. This may explain why the hook length is not strictly controlled but has a relatively broad distribution. The third model is exemplified by InvJ of *Salmonella*, which is required to stabilize the conformation of the socket located within the basal part of the NC (Marlovits *et al*., 2006; Sani *et al*., 2007b). This socket, located within the lower rings of the basal body (Galan and Wolf-Watz, 2006; Marlovits *et al*., 2006; Sani *et al*., 2007b), is hypothesized to function as an anchoring platform for the assembly of the inner rod, whose completion would result in the firm anchoring of the needle to the base. This triggers conformational changes that will consequently reprogram the secretion apparatus to halt secretion of the needle and inner rod proteins.

We have previously shown that the length of the MxiSpa T3SA needle substructure is fairly well controlled at approximately 50 nm by the Spa32 protein (Magdalena *et al*., 2002). Here, we address the question of whether Spa32 also functions as a molecular ruler in the control of the needle length by examining the phenotypes of Spa32 variants obtained by deletions in the N-terminus, central and C-terminus part of the full-length *spa32* gene or by insertion of the YscP's ruler domain. Generated Spa32 variants were tested for their capacity to restore needle length control, Ipa proteins secretion and HeLa cells invasion. Moreover, we identified a molecular interaction between Spa32 and Spa40, a component of the type III secretion machinery.

Results

Functional analysis of Spa32 domains in Ipas secretion and HeLa cell invasion

In a previous study, we reported that Spa32 is required for Ipa proteins secretion upon T3SA induction (Magdalena *et al*., 2002). To identify domains of Spa32 involved in secretion, in-frame deletions within *spa32* gene were constructed on the pMJ8 plasmid encoding His-Spa32 (see *Experimental procedures*; Table S1; Fig. 1A). pMJ8 was previously shown to restore the wild-type secretion phenotype when expressed in Δ*spa32* (Magdalena *et al*., 2002). His-Spa32 variants lacking either the N-terminal domain residues: Δ2-10 (pAB34 encoding D1 protein), Δ2–36 (pAB36: D2), Δ37–94 (pAB66: D3); central domain residues: Δ94–187 (pAB35: D4), Δ94–159 (pAB47: D5), Δ130–187 (pAB46:D6), Δ130–159 (pAB38: D7), Δ206–280 (pAB65: D8); or the C-terminal domain residues Δ239–292 (pAB37: D9) or Δ264–292 (pAB39: D10) were constructed, and production of His-Spa32 variants (D1 to D10) was assessed by Western blot using the anti-His or

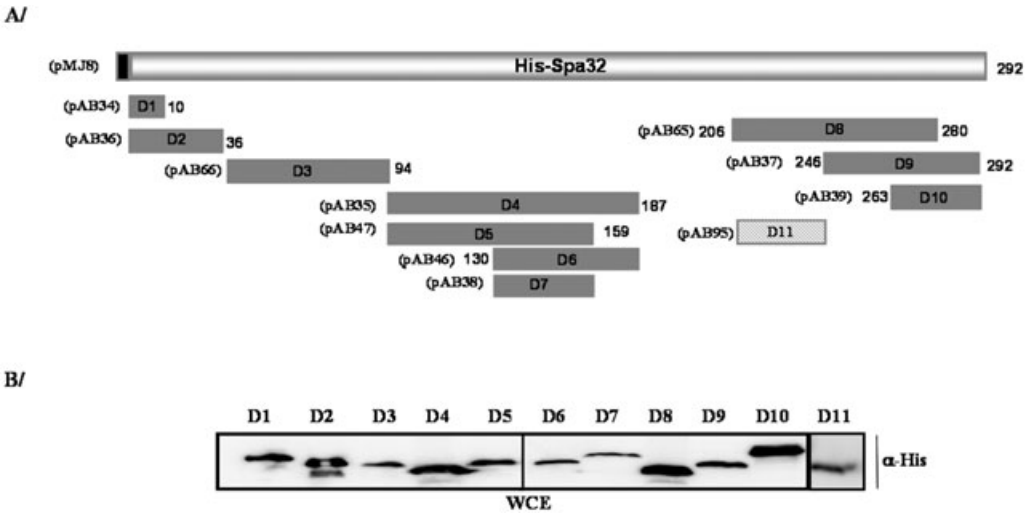

Fig. 1. Construction and production of His-Spa32 truncated derivatives.
A. Schematic representation of the deletions made within *his-spa32* gene harboured on the pMJ8 plasmid. These plasmids were constructed by PCR as indicated in *Experimental procedures*. Dark boxes represent the regions deleted within the Spa32 protein. Position of amino acid residues and the plasmid names are indicated. D1 to D10 represent the name given to truncated His-Spa32 variants.
B. Production of truncated His-Spa32 variants. Whole-cell extracts of Δ*spa32* harbouring plasmids encoding D1 to D11 were prepared from bacteria grown to log phase. Equivalent amounts, 0.3 OD_{600} of each sample, were loaded on SDS-PAGE and probed using the anti-His monoclonal antibody.

the anti-Spa32 antibodies (Fig. 1B and data not shown). Next, the His-Spa32 variants were analysed for their capacity to restore the wild-type secretion of Δ*spa32*. Bacteria grown to exponential growth phase were incubated with Congo red to induce Ipa proteins secretion (see *Experimental procedures*). Cultures supernatants of Δ*spa32* expressing His-Spa32 variants were analysed by SDS-PAGE, Coomassie blue-stained or immunoblotted using monoclonal antibodies (Mab) against IpaC. As a control we loaded proteins from the supernatant of Δ*spa32* expressing the entire His-Spa32 protein. As shown in Fig. 2A, secretion of IpaC was seen only in Δ*spa32* strain expressing parental His-Spa32, D3 and D7 but not from Δ*spa32* expressing D1, D2, D4 to D6 and D8 to D10 proteins. The lack of secretion was not due to the lack of IpaC synthesis by the various strains (Fig. 2B).

To investigate the ability of Δ*spa32* strains expressing His-Spa32 variants to enter HeLa cells, we performed quantitative gentamicin protection assay as described in

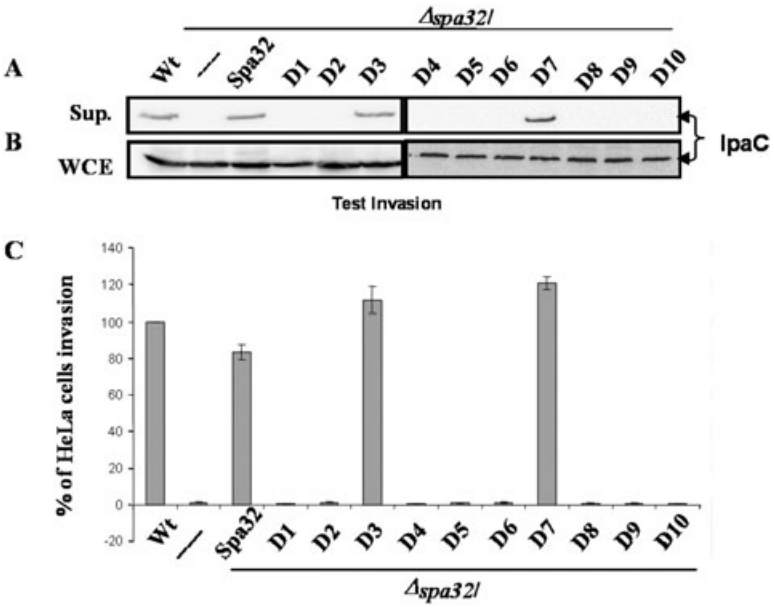

Fig. 2. IpaC secretion and invasion of HeLa cells by His-Spa32 derivatives.
A. IpaC production and secretion. Whole-cell extracts of Δ*spa32* strain harbouring pAB plasmids encoding D1 to D10 were prepared from bacteria growth to log phase. An OD_{600} of 0.3 of each sample was loaded on SDS-PAGE and probed using the anti-IpaC monoclonal antibody. For the supernatant, bacteria grown to log phase were centrifuged, and the pellet was incubated with Congo red to induce proteins secretion via the T3SA. Secreted proteins were then separated on SDS-PAGE and immunoblotted using the IpaC specific Mab.
B. Invasion of HeLa cells by the Δ*spa32* strain expressing His-Spa32 or its derivatives D1 to D10. *Shigella* strains grown to log phase were incubated with HeLa cell cultures. After cells lysis, bacterial counting was performed by spreading bacteria on plates containing selective antibiotics.

the *Experimental procedures*. As indicated in Fig. 2C, quantification of the number of intracellular bacteria clearly demonstrates that most His-Spa32 variants, except parental His-Spa32, D3 and D7, were not able to restore the entry defect of Δ*spa32.* This indicates that residues 36–94 (D3) and 130–159 (D7) are dispensable in both Ipa proteins secretion and HeLa cell invasion.

Needle length is not controlled by a molecular ruler mechanism

Electron microscopy examination of wild-type strain shows that it possesses needles of normal length that ranges between 34 and 90 nm, with a peak around 45 nm (Fig. 3). Most of the needles were attached to the surface of the bacteria. Our measurements were based on attached needles, but a comparison of detached and attached needles did not show any significant differences (data not shown). In contrast, examination of Δ*spa32* shows that the needle length is distributed over a broad range from 100 to 900 nm, with a peak around 314 nm (Fig. 3). Complementation of the Δ*spa32* by pMJ8, expressing parental His-Spa32, restored the length to a range between 18 and 78 nm with a peak at around 44 nm, similar to wild-type phenotype (Fig. 3). To test whether Spa32 deletions affect needle length, Δ*spa32* strains expressing the 10 His-Spa32 variants (D1 to D10) were examined by EM. We found that mutations in both N-terminal (D1 or D2) and C-terminal (D9 or D10) domains of Spa32 affected needle length control, with production of shorter needles ranging between 152 and 217 nm compared with Δ*spa32* (314 nm) (Table 1). This indicates that both Spa32 terminal regions are required for precise length control. When Δ*spa32*-expressing His-Spa32 variants with internal mutations were examined, only D3 and D7 proteins restored wild-type needle length, 45.6 and 46 nm, respectively, while D4, D5, D6 and D8 programmed needles of 165, 194, 210 and 147 nm respectively (Fig. 3D and Table 1). This indicates that needle length is not proportional to the size of the Spa32 protein.

Spa32 interacts, via residues 206–246, with the C-terminal domain of Spa40

FliK was shown to interact with the soluble carboxyl-terminal domain of FlhB ($FlhB_c$) (Minamino and Macnab, 2000). This interaction plays a crucial role in the switch from hook to filament secretion in the flagellum system. To test whether Spa32 interacts with *Shigella*'s FlhB counterpart (Spa40), we constructed plasmid pAB51 encoding GST-Spa40CT. The latter contains GST fused to the cytoplasmic Spa40 domain composed of residues 205–342. Soluble extracts of Δ*spa32* producing parental His-Spa32 were incubated with GST-Spa40CT or GST bound to glutathione sepharose beads, and proteins retained on the beads were eluted with gluthanione. SDS-PAGE analysis of eluted proteins indicated that His-Spa32 interacted with GST-Spa40CT but not with GST alone (Fig. 4A). To investigate the interaction of GST-Spa40CT with native Spa32, beads carrying GST-Spa40CT were incubated with a concentrated culture supernatant preparation of wild-type *S. flexneri* containing Spa32 (Magdalena *et al*., 2002). Analysis of eluted fractions by Western blot using an anti-Spa32 polyclonal antibody indicated that native Spa32 binds to GST-Spa40CT (Fig. 4B). As a control, IpaD, which is present in the culture supernatant fraction, does not interact with GST-Spa40CT (Fig. 4B).

To localize the domain of Spa32 that interacts with Spa40, we performed a similar GST pull-down assay by taking advantage of the 10 His-Spa32 variants. Soluble *E. coli* extracts producing His-Spa32 parental or variant proteins were incubated with GST-Spa40CT or GST alone bound to glutathione sepharose. Analysis of eluted fractions indicates that GST-Spa40CT was able to interact, although at different levels, with the five His-Spa32 variants D2, D3, D4, D9 and D10, which are the most representative Spa32 truncated derivatives (Fig. 4C). However, variant D8, in which residues 206–280 were deleted from His-Spa32, was no longer able to interact with GST-Spa40CT (Fig. 4C). The absence of interaction was not due to the lack of D8 production, as it was produced at similar levels compared with wild-type His-Spa32 (Fig. 4C). The fact that D9 contains a deletion of residues 246–292 but still interacts with Spa40CT although at reduced level, and that D8 has residues 206–280 deleted, and cannot interact with Spa40CT, suggests that residues 206–246 are required for Spa40 binding. To test this hypothesis, we constructed variant D11 by deleting residues 206–246. Here we show that this Spa32 variant, although expressed, was no longer able to interact with Spa40CT (Fig. 4C). Thus, we conclude that the Spa32 domain, encompassing residues 206–246, is essential for Spa40 binding. Moreover, we found that D11 was unable to restore the Δ*spa32* defect in HeLa cell invasion, Ipa proteins secretion or needle length control (data not shown and Fig. 4D).

Spa32 is interchangeable with Salmonella *InvJ and* Y. enterocolitica *YscP*

The three proteins Spa32, InvJ of *Salmonella* and YscP of *Y. enterocolitica* share very low sequence similarity and are required for needle length control of their respective T3SA (Fig. 5). To test whether the expression of InvJ or YscP could complement the lack of Ipas secretion of Δ*spa32*, we constructed pDR1 and pAB75; plasmids derivatives of pTZ18R vector that constitutively express

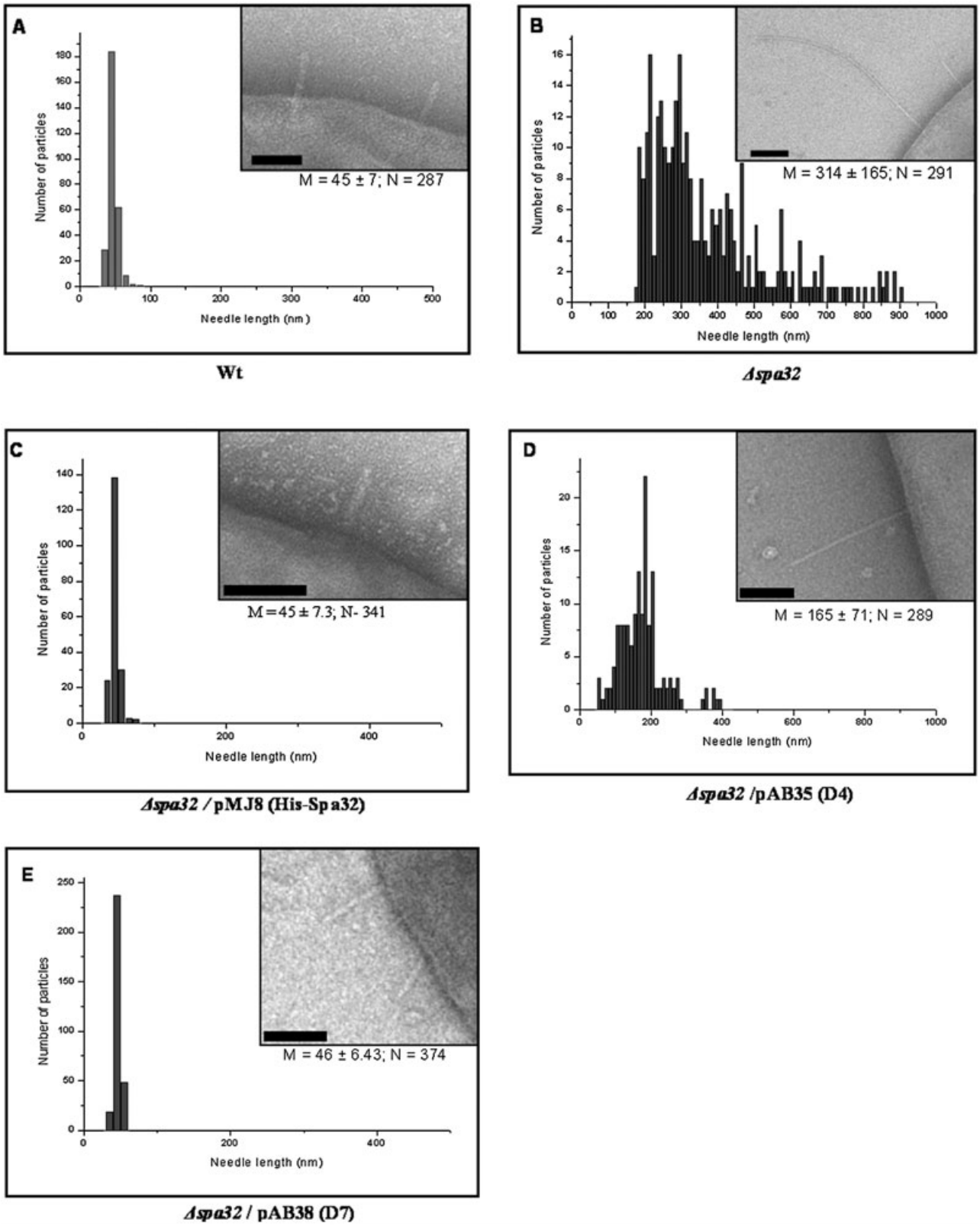

Fig. 3. Effects of *spa32* deletions on needle length. Histogram of needle length measurements and electron micrographs of *S. flexneri* wild-type (A); Δ*spa32* mutant expressing needles of random length that sometimes span 0.9 μm (B); Δ*spa32* mutant complemented with pMJ8 (His-Spa32) showing restoration of wt phenotype (C); D4 deletion variant producing long needles (D); and D7 deletion variant producing needles of wt phenotype length (E). M, median with standard deviation (in nm); N, number of needle particles measured. Scale bars, 50 nm.

Table 1. Needle length control by Spa32 and its derivatives.

Strains	# of aa	M	SD	N
Wt	292	**45**	7	287
Δ*spa32*	90[a]	314	165	291
Δ*spa32*+ His-Spa32	292	**44**	8	341
D1	282	187	85	177
D2	256	152	82	233
D3	233	**45.6**	5	303
D4	198	165	71	289
D5	226	194	87	116
D6	234	210	84	257
D7	262	**46**	11	554
D8	207	147.3	68	173
D9	237	183	103	119
D10	262	182	91	152
D11	250	182	75	190
YscP	515	**53.7**	13	131
InvJ	336	**46.2**	13	174
Spa32Ω	396	97	36	192

a. Spa32 N-terminal residues that are still produced by the Δ*spa32* mutant (Magdalena *et al*., 2002).
Number in bold indicates when the length of the needle is fairly controlled around 50 nm. Spa32Ω corresponds to the hybrid $Spa32_{1-145}YscP_{202-306}Spa32_{146-292}$ protein. The number underlined in the lower part of the Table indicates that the length of the needle is slightly elongated (twofold) compared with the wild-type strain.
Needle length measurements: # of aa, number of amino acids of Spa32; M, median of the lengths (nm); SD, standard deviation (nm); N, number of needle particles measured.

InvJ of *Salmonella* or YscP of *Y. enterocolitica*. These plasmids were introduced into Δ*spa32* and the resulting strains were first checked for their ability to secrete IpaB and IpaC. Induced culture supernatants of Δ*spa32* strain expressing InvJ or YscP were analysed by SDS-PAGE, Coomassie blue stained or immunoblotted using Mab against IpaB and IpaC. Interestingly, we found that both InvJ and YscP restored IpaB and IpaC secretion by Δ*spa32* (Fig. 6A). Likewise, ectopic expression of InvJ and YscP in Δ*spa32* restored the entry into HeLa cells (Fig. 6B). Lastly, we found that Δ*spa32* strains expressing InvJ or YscP also restored the capacity of Δ*spa32* to control needle length at 46 and 53 nm respectively (Table 1 and Fig. 6C and D). We conclude from these experiments that Spa32 function is interchangeable with InvJ and YscP homologues.

To investigate YscP or InvJ interaction with Spa40CT, we constructed pAB103 and pAB104 two pTZ18R derivative plasmids encoding His-YscP and His-InvJ and performed GST-Spa40CT pull-down assay. We found that neither of the two hybrid proteins was able to interact with GST-Spa40CT (data not shown). This result can be associated to the reduced amounts of His-YscP and His-invJ constitutively expressed from the *lacZ* promoter of the pTZ18R vector (data not shown). To test further the interaction of InvJ and YscP with GST-Spa40CT, in a similar condition used to detect His–Spa32 interaction, we constructed two plasmids, derivative of the pQE60 vector, producing InvJ-His (pCAK-J) and YscP-His (pCAK-P). Soluble extracts of *E. coli* producing InvJ-His and YscP-His were incubated with GST-Spa40CT or GST bound to glutathione sepharose beads, and proteins retained on the beads were eluted with gluthanione. SDS-PAGE analysis of eluted proteins indicated that InvJ-His and YscP-His, like His-Spa32, interacted with GST-Spa40CT but not with GST alone as a control (Fig. 6E).

We conclude from these results that InvJ or YscP can fully replace Spa32 in all tested assays including proteins secretion, Hela cells invasion, needle length control and Spa40 interaction.

The insertion of the $YscP_{202-306}$ ruler domain of Yersinia *within Spa32 affects the needle length of* Shigella *but not the secretion and the invasion processes*

It was reported that a central domain of YscP encompassing residues 202–306 contains a ruler domain (Journet *et al*., 2003). When this domain was duplicated in YscP of *Y. enterocolitica* itself or inserted within FliK, the length of the needle or the hook was enhanced (Journet *et al*., 2003; Shibata *et al*., 2007). To test whether the insertion of the $YscP_{202-306}$ ruler domain within Spa32 affect the MxiH needle length, we constructed plasmid pAB106 expressing $Spa32_{1-145}YscP_{202-306}Spa32_{146-292}$ (Spa32Ω) by fusing in-frame residues 202–306 of YscP between residues 145 and 146 of Spa32 (Fig. 7A). To avoid any effect on Spa32 function, the ruler domain was inserted within the central part of the D7 domain, which is disposable for Spa32 functioning (Figs 2 and 7A). Spa32Ω was able to complement the lack of secretion and invasion of the *spa32* mutation in a comparable manner to the wild-type strain (Fig. 7B and C), indicating that the insertion of the YscP's ruler domain does not affect the function of Spa32. To test whether the insertion of the YscP's ruler domain affect needle length, Δ*spa32* strains expressing Spa32Ω variant were examined by EM and were found to program needles of approximately 97 nm (Fig. 7D). Comparatively, the needles are controlled at wild-type level by the unmodified Spa32 protein (45 nm). We conclude from these results that the insertion of the ruler domain of YscP within Spa32 enhanced the length of the needle by twofold.

Discussion

Pathogenic bacteria use a type III secretion nanomachine to deliver virulence proteins into the cytosol of their eukaryotic host cells. Most NCs possess a stiff needle-like structure of a genetically defined length. The needle may be required for triggering T3S, and its length could have

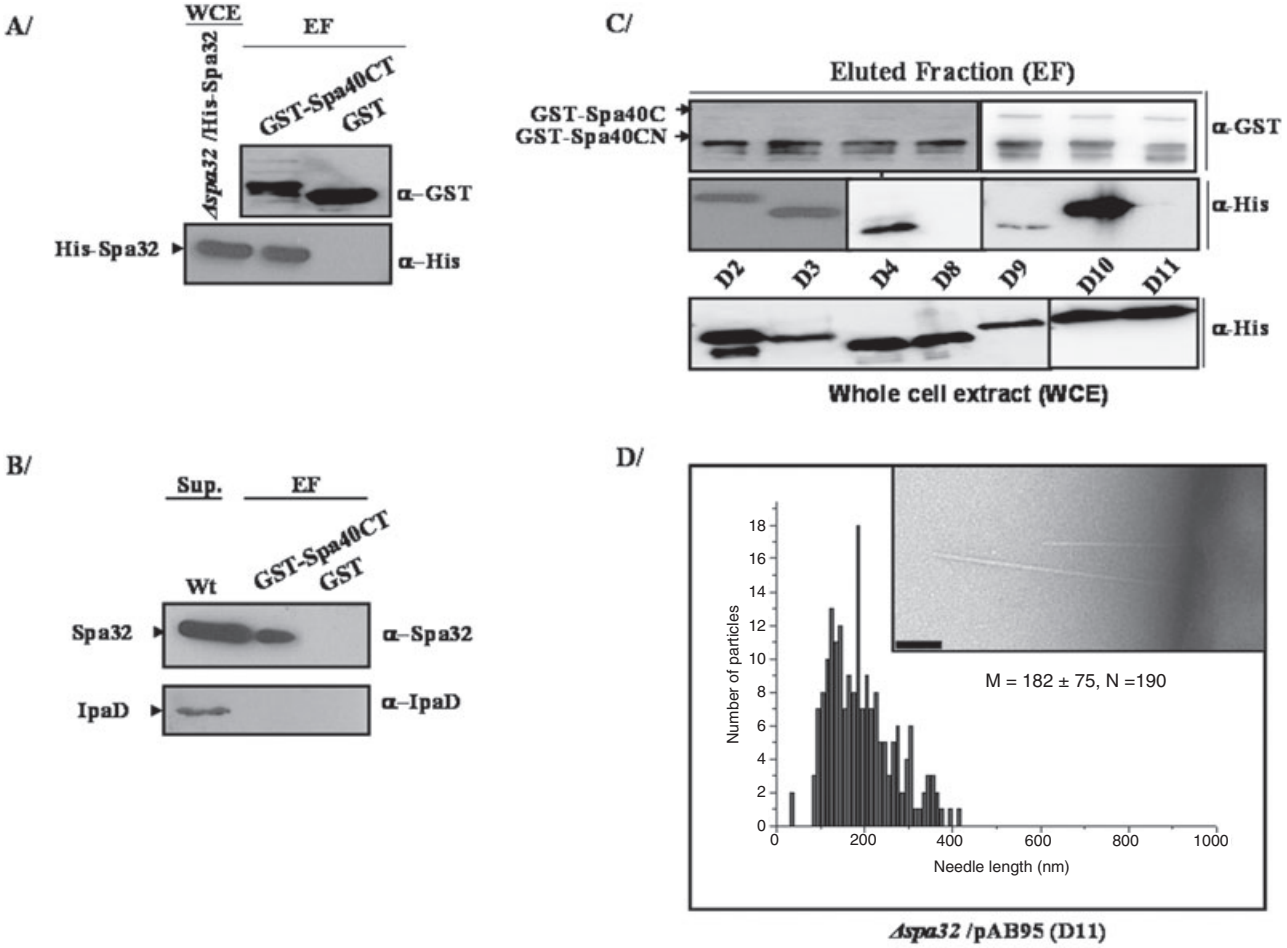

Fig. 4. Spa32 interacts with the integral inner-membrane protein Spa40. Soluble *E. coli* extracts producing His-Spa32 parental or variant proteins were incubated with GST-Spa40CT or GST alone bound to glutathione sepharose.
A. Analysis of eluted fractions (EF) separated on SDS-PAGE and probed with anti-GST (to detect GST derivatives) or Mab anti-His (to detect His-Spa32 derivatives) indicates that GST-Spa40CT was able to interact with parental His-Spa32 but not with the GST alone.
B. Spa40CT interacts with native Spa32. Soluble proteins from the supernatant of wild-type *Shigella* were incubated with GST-Spa40CT or GST alone bound to glutathione sepharose. EF were separated on SDS-PAGE and probed with the polyclonal antibodies anti-Spa32 or anti-IpaD.
C. Identification of the minimal Spa32 domain required for Spa40 binding. Soluble *E. coli* extracts producing the most representative His-Spa32 variant proteins (D2-D4, D8-D10) or variant D11 were incubated with GST-Spa40CT bound to glutathione sepharose. Analysis of EF separated on SDS-PAGE and probed with anti-GST (to detect GST derivatives) or Mab anti-His (to detect His-Spa32 derivatives).
D. Histogram of needle length measurements and electron micrographs of *S. flexneri* Δ*spa32* complemented with plasmid pAB106.

evolved to match specific structures at the bacterial and host cell surfaces. Molecular rulers are generally involved in length determination of such long macromolecules (Cornelis, 2006). The importance of needle length control of the T3SS was previously emphasized by two major reports by West *et al*. (2005) and Mota *et al*. (2005). West *et al*. demonstrated that shortening the lipopolysaccharide molecule by around half in *Shigella* enhances T3SS invasion function by allowing the T3SS to be more exposed on the bacterial surface. Mota *et al*. found that a minimal needle length was required for efficient functioning of the *Y. enterocolitica* injectisome. It was later shown that this minimal needle length correlate with the length of the YadA adhesin on the bacterial surface (Cornelis, 2006).

The goal of this study was to determine how Spa32 acts to regulate overall MxiH needle length. We characterized the function of 11 Spa32 variants with deletions within the N-terminal domain, the central domain or at the C-terminus by testing Ipas secretion, HeLa cell invasion and needle length control. We showed that with the exception of residue deletions 36–94 (D3) and 130–159 (D7), which still generate functional His-Spa32 proteins, all other Spa32 variants were not functional (Fig. 8). Proteins truncated within the first 10 (D1) or 36 residues (D2), which contain the type III predicted secretion signal, or

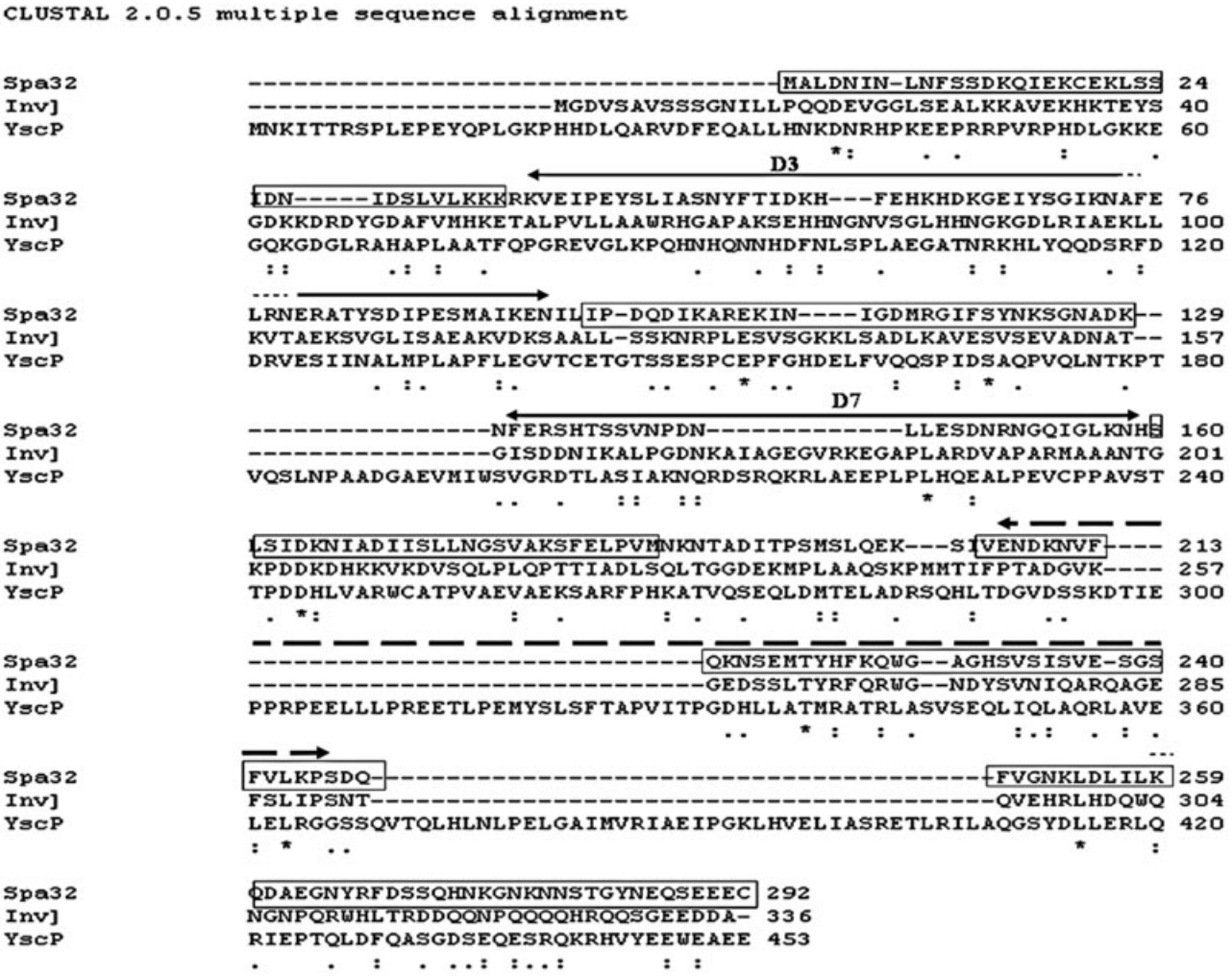

Fig. 5. Sequence alignment of the Spa32 family using Clustal (2.0.5). Alignment of the amino-acids sequence of Spa32 (*S. flexneri*) and InvJ (*Salmonella*) and YscP (*Y. enterocolitica*). Residues that are identical are indicated by stars, while similar residues are indicated by simple or double dots. The boxes represent domains of Spa32 that are required for its function. The D3 and D7 domains that are dispensable for Spa32 function are indicated by horizontal arrows. The D11 domain that is required for Spa32 binding to Spa40 is represented in the lower part by an horizontal dashed arrow shown in bold.

with a deletion of the last 29 residues (D10) were unable to control the length of the needle, even though the needles produced were shorter than with Δ*spa32*. Similarly, large truncations within the internal region, D4 or D6, produced similar needle length as variants with N-terminus and C-terminus truncations. In contrast, single deletions of 58 residues in D3, or 29 residues in D7, produced needles of comparable size to the wild-type strain. Collectively, our data suggest that Spa32 does not act as a molecular ruler to regulate the needle length because mutants with large deletions within Spa32 do not produce shorter needles than those generated by variants with minimal deletions.

Length of the needle or hook is regulated at around 50–55 nm in *Shigella* and *Salmonella* and around 60 nm in *Y. enterocolitica*, by proteins that have varying sizes. Spa32 contains 292 residues, while InvJ, YscP and FliK are composed of 336, 515 and 409 residues respectively. We show that Spa32 and InvJ or YscP are functionally interchangeable. We confirmed the complementation reported of the Δ*spa32* by InvJ (Tamano *et al.*, 2002), and showed in addition that YscP can replace Spa32 functions. The latter result contrasts with the lack of Δ*spa32* complementation by YscP reported by Tamano *et al.* (2002). While YscP contains 117 residues more than Spa32, the length of the needle, however, was not proportionally longer when it was produced in Δ*spa32*. In contrast, the insertion of YscP's ruler domain within Spa32 does not affect the Spa32 function but produced needles whose length were enhanced twice compared with wild-type strain (97 versus 45 nm). This finding corroborates previously reported data obtained with YscP or

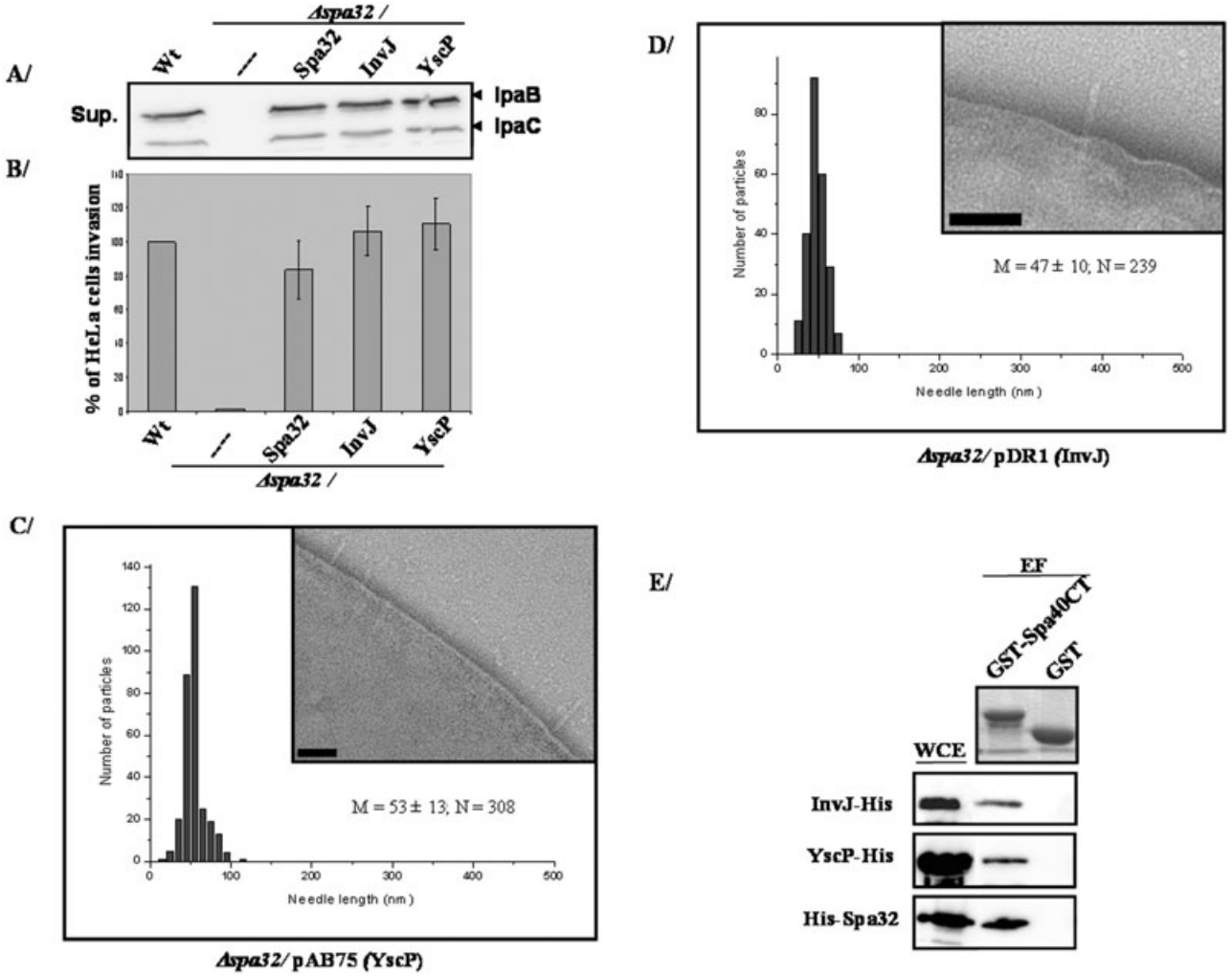

Fig. 6. Spa32 is interchangeable with *Salmonella* InvJ and *Y. enterocolitica* YscP. Bacteria grown to log phase were centrifuged and the pellet was incubated with Congo red to induce proteins secretion via the T3SA (see *Experimental procedures*).
A. Secreted proteins were then separated on SDS-PAGE and immublotted using IpaB and IpaC Mabs.
B. Hela cells invasion by the *spa32* mutant expressing InvJ from *Salmonella* or YscP from *Y. enterocolitica*. *Shigella* strains grown to log phase were incubated with HeLa cells culture (see *Experimental procedures*). After cells lysis, bacterial counting was performed by plating bacteria on plates containing selected antibiotics.
C and D. Histograms of needle length measurement and electron micrographs of Δ*spa32* complemented with InvJ or YscP producing normal needles. M, median of the lengths (nm); N, number of needles measured. Scale bars, 50 nm.
E. InvJ and YscP interact with Spa40. Soluble *E. coli* extracts producing YscP-His and InvJ-His were incubated with GST-Spa40CT or GST alone bound to glutathione sepharose. Analysis of eluted fractions (EF) separated on SDS-PAGE was done by Coomassie blue staining (upper part) or by probing with a Mab anti-His (lower part).

FliK fused to the YscP ruler domain that produced elongated needle or hook substructures. Thus, in contrast to Spa32 and probably to FliK, YscP functions as a molecular ruler because of the presence of its ruler domain (Journet *et al*., 2003).

In a previous work by Shibata *et al*. (2007), it was reported that FliK contains three ruler domains, which are dispensable for its function (Fig. 1S). When compared with Spa32, one of these FliK domains that match the region deleted in D3 variant remains functional. However, in contrast to FliK, D5 and D6 variants deleted from the sequence that match the two other ruler domains of FliK abolished Spa32 function (Figs. 2 and 1S). We conclude that despite their similarity, both Spa32 and FliK proteins might have their own functional specificity within their corresponding T3SS.

We identified a molecular interaction between Spa32, InvJ or YscP and the soluble cytoplasmic domain of Spa40, a well-conserved inner-membrane T3S component whose crystal structure was recently reported (Deane *et al*., 2008). To our knowledge, this is the first report of such an interaction in the T3SS besides the

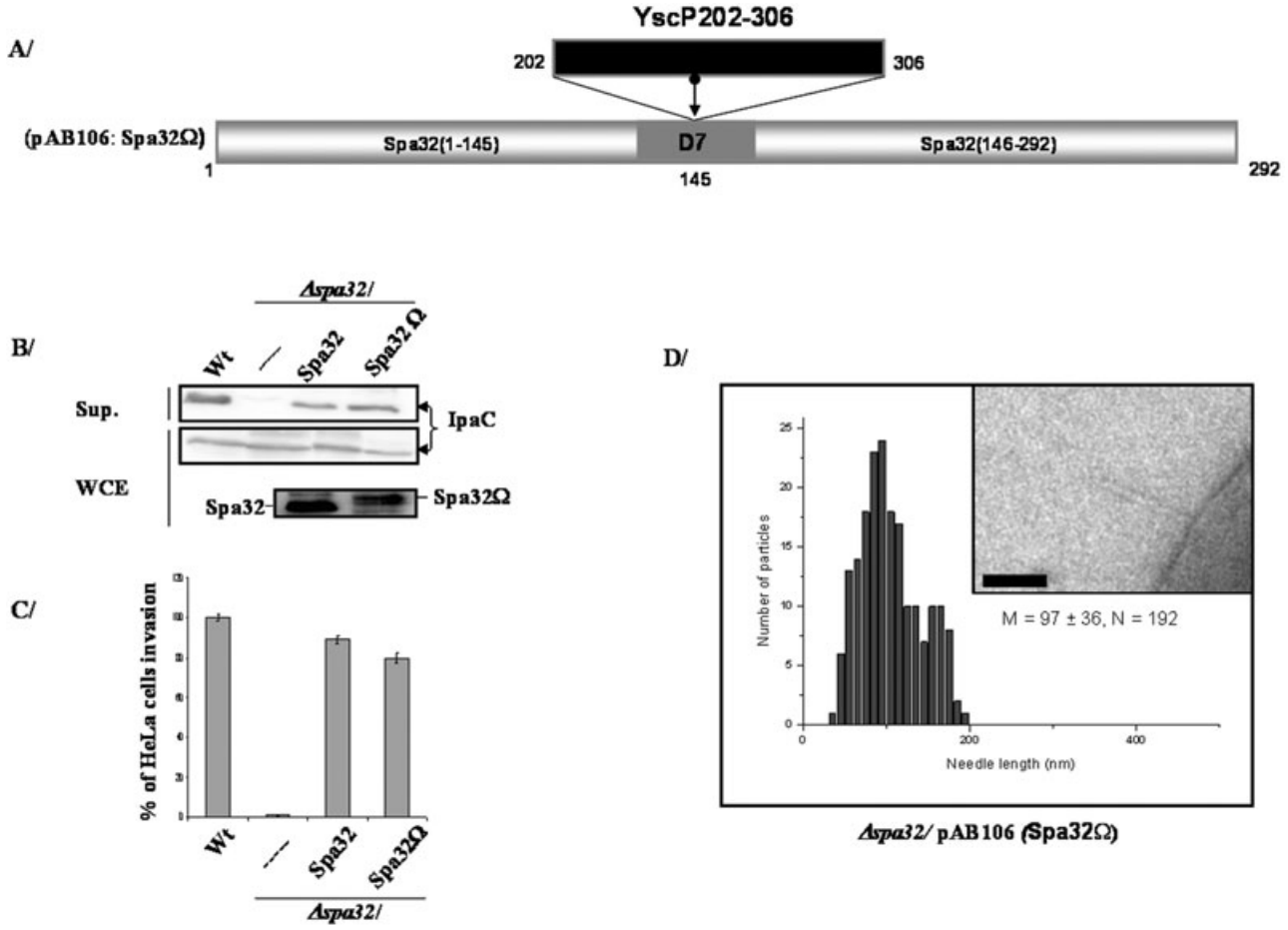

Fig. 7. The insertion of the ruler domain of YscP within Spa32 enhances needle length but does not affect secretion and Hela cells invasion.
A. Schematic representation of the plasmid pAB106 encoding Spa32Ω: the ruler domain of YscP (black box) from residues 202–306 was inserted in-frame between residues 145 and 146 of Spa32.
B. Bacteria strains: wild-type, Δ*spa32* alone or complemented either with the unmodified Spa32 or Spa32Ω were grown to log phase, centrifuged and the pellet was incubated with Congo red to induce proteins secretion via the T3SA (see *Experimental procedures*). Whole-cell extract and secreted proteins were then separated on SDS-PAGE and immublotted using an anti-IpaC Mab or an anti-Spa32 polyclonal antibodies.
C. Hela cells invasion by the *spa32* mutant expressing Spa32Ω. *Shigella* strains grown to log phase were incubated with HeLa cells culture (see *Experimental procedures*). After cells lysis, bacterial counting was performed by plating bacteria on plates containing selected antibiotics.
D. Histograms of needle length measurement and electron micrographs of Δ*spa32* complemented with Spa32Ω making slightly elongated needles. M, median of the lengths (nm); N, number of needles measured. Scale bars, 50 nm.

flagellum. Several studies have reported the importance of the FliK/FlhB interaction in mediating the switch in substrate specificity (from hook protein to flagellin) upon completion of hook assembly (Minamino and Macnab, 2000). Comparatively, in *Yersinia*, there is indirect evidence that suggests a dual role for YscP/YscU, in the switch from the needle YscF secretion to that of Yops (Edqvist *et al*., 2003). Taking advantage of truncated Spa32 variants, we identified the Spa32 domain required for Spa40 binding, which is located between residues 206 and 246. Interestingly, protein D11, lacking residues 206–246, was not functional, suggesting that the Spa32/Spa40 interaction is crucial for the switch from MxiH to Ipa proteins secretion. Sequence analysis revealed that residues 206–280, encompassing the Spa40 interaction domain, share features with the previously described T3S4 switch domain of YscP and FliK (Agrain *et al*., 2005; Minamino *et al*., 2006; Fig. 8; data not shown). FliK variants, lacking the T3S4, were not able to interact with $FlhB_c$ and were not functional (Minamino *et al*., 2004). Thus, one could consider that Spa32's binding to Spa40 may serve to regulate the conformation of Spa40CT in the cytosol of the bacterial cell. Likewise, the controlled switch in the flagellum system is believed to be mediated by conformational changes in the structure of $FlhB_c$.

Spa32 variants such as D1, D2 and D4, which still contain the T3S4 domain, were not functional. This contrasts with reported data on YscP variants harbouring

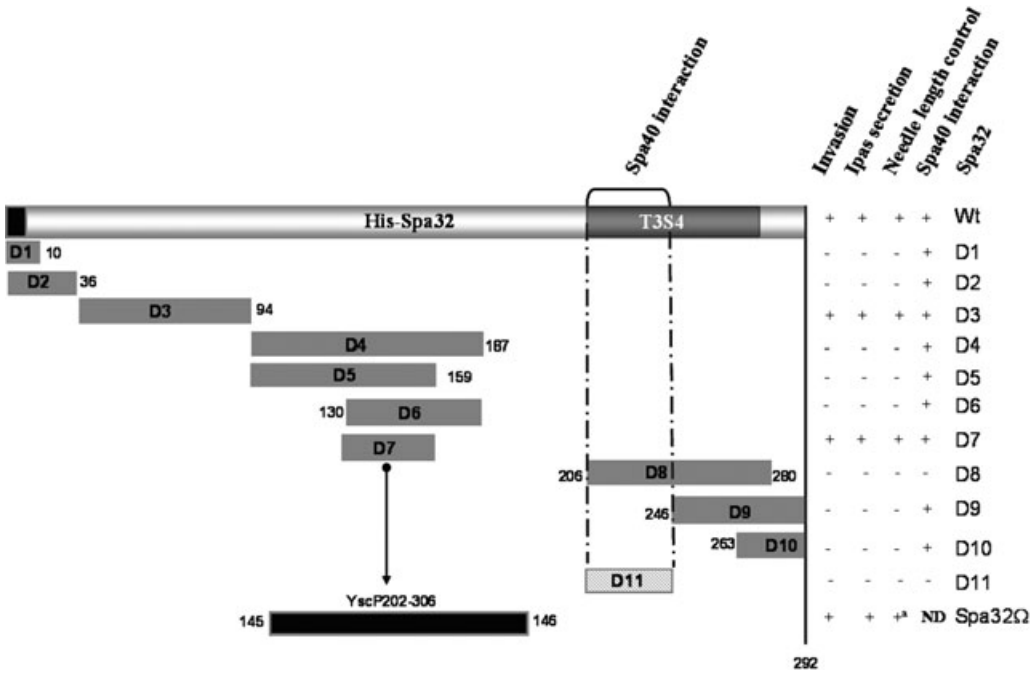

Fig. 8. Summary of the phenotypes obtained with His-Spa32 derivatives. All His-Spa32 variants (D1 to D11) were tested for their ability to restore the capacity of the Δ*spa32* mutant: (i) to invade HeLa cells; (ii) to secrete the Ipa proteins; (iii) to control the needle length; and (iv) to interact with the T3S component Spa40. The symbol '+' indicates restoration and '–' indicates that the variants do not restore the studied phenotypes. ND, not tested. Residues 260–280 of Spa32 share features of the type III secretion switch domain also called T3S4, which is conserved in YscP and FliK homologues. Dashed box, which is part of the T3S4, represents the identified Spa32 minimal domain required for Spa40 binding. Dark Box represents the YscP's ruler domain that was inserted between residues 145 and 146. [a]The length of the needle is doubled in the Δ*spa32* mutant expressing Spa32Ω (97 versus 45 nm in the wild-type strain).

each the T3S4 domain, which were still able to switch to Yop secretion even though they have lost their capacity to control the YscF needle length (Agrain *et al*., 2005). Here, we demonstrate that needle length control and the switch to Ipa proteins secretion are coupled in *Shigella*, similar to hook control by FliK (Williams *et al*., 1996). Accordingly, our data are most likely in agreement with the molecular tape measure model previously reported for FliK (Moriya *et al*., 2006), rather than the molecular ruler model of YscP (Journet *et al*., 2003). When $FliK_N$ is within the central channel of the growing hook-basal body structure, it temporarily binds to the hook-cap. Secretion is then paused to allow $FliK_C$ to interact with $FlhB_C$, altering the export specificity from hook to filament. When the hook is very short, $FliK_C$ is not in close proximity to $FlhB_C$ during the secretion pause, and a successful interaction does not occur efficiently. In contrast, when the hook length is within the pre-set range, $FliK_C$ is in the correct position to interact with $FlhB_C$, causing its conformational change that results in the switch of export specificity. According to this model, Spa32 molecules deleted in the N-terminus domain (D1 and D2), lacking the T3S signal, are probably no longer able to interact with other T3S components required for Spa32 export to the bacterial surface. Likewise, Spa32 variants with deletions of the C-terminal domain (D9 and D10) are not well placed in the needle and so cannot interact at the right time with Spa40CT, even if the Spa32 domain that interacts with Spa40 is physically present. Consequently, D1, D2, D9 and D10 mutants still produce very long needles and do not switch from MxiH to Ipa proteins secretion. Proteins D8 and D11 are probably correctly placed in the needle structure but they lack the Spa40 interaction domain so, in this way, they also cannot switch to Ipas secretion. Proteins D4, D5 and D6 were not functional, although they do contain the C- and N-terminus domains as well as the Spa40 interacting domain. We hypothesize that two additional domains of Spa32, corresponding to residues 94–130 and 159–187, might be required for an additional Spa32 function, probably by an interaction with other as yet unidentified T3S components. Lastly, proteins D3 and D7, which remain fully functional, have the two anchors points, the 94–130 and 159–187 domains, and the entirety of the T3S4 domain to enable them to interact with Spa40.

In conclusion, our results indicate that Spa32 does not serve as a molecular ruler in determining the length of the needle. It appears instead that Spa32 may function as a molecular tape measure. Because deletions affecting both N- and C-termini of Spa32 lead to a loss of length control, we hypothesize that the two ends of Spa32 act as anchors. One end of Spa32 would be attached to the basal body, probably by its interaction with Spa40, leading

to the formation of the socket and the other end would be connected to the growing tip of the needle. As Spa40/Spa32, YscU/YscP, SpaS/InvJ and FlhB/FliK protein pairs have counterparts in all bacteria with flagella and/or T3SSs, one can consider that mechanisms involved in regulation of inducible secretion, hook length control, and switching to filament assembly share common regulatory pathways.

Experimental procedures

Bacterial strains and growth media

Shigella flexneri strains are derivatives of the wild-type strain M90T (serotype 5) (Allaoui *et al*., 1992). The M90T-Sm (Sm^r) and the *spa32* mutant (Δ*spa32*) have been described previously (Allaoui *et al*., 1992; Magdalena *et al*., 2002). *Escherichia coli* strains are K-12 strain derivatives. The M15 strain harbouring the pREP4 plasmid was transformed with pQE30 derivatives. Bacteria were grown in tryptic casein soy broth (TSB) (Sigma) at 37°C. Antibiotics were used at the following concentrations: ampicillin 100 μg ml^{-1}, kanamycin 50 μg ml^{-1}, streptomycin 100 μg ml^{-1} and gentamicin 50 μg ml^{-1}.

Plasmids construction

Deletions were generated by inverse polymerase chain reaction (iPCR) using the pMJ8 (pQE30-Spa32; Magdalena *et al*., 2002) plasmid as template, followed by a ligation. pMJ8 derivatives carrying deletion mutations on *his-spa32* gene are listed in Table S1. Primers used is this study are listed in Table S2. pMJ8 derivatives were first checked by DNA restriction analysis and all *spa32* deletions were further confirmed by DNA sequencing. Production of pMJ8 derivatives plasmid encoding His-Spa32 (full or truncated proteins) was checked by immunoblot using the His-tag monoclonal antibody. pMJ8 derivatives were further introduced into Δ*spa32* to study the virulence properties of the resulting strains. Plasmid pDR1 expressing the *Salmonella* InvJ protein was constructed by cloning *Eco*RI–*Sma*I *invJ* PCR DNA digested product, obtained using InvJs and InvJas primers, into the corresponding sites of pTZ18 vector. Plasmid pAB75 expressing YscP from *Yersinia enterocolitica* was constructed by cloning *Eco*RI–*Sma*I *yscP* PCR DNA digested product, obtained using YscP1s and YscPas primers, into the corresponding sites of the pTZ18 vector. In both pDR1 and pAB75, the constitutive expression of InvJ and YscP is under the control of the *plac* promoter of the vector. Plamsid pAB106 was constructed by inserting in-frame a 312 bp PCR DNA fragment encoding residues 202–306 of YscP between residues 145 and 146 of Spa32 (Fig. 7). This plasmid encodes the chimerical $Spa32_{1–145}YscP_{202–306}Spa32_{146–292}$ protein also called Spa32Ω. Plasmids pAB103 and pAB104 expressing His-YscP and His-InvJ were constructed by inserting *his-yscP* and *his-invJ* PCR DNA fragments into pTZ18R vector. Plasmids pCAK-P and pCAK-J expressing YscP-His and InvJ-His were constructed by inserting *yscP* and *invJ* PCR DNA fragments into pQE60 expression vector.

Plasmid pAB51, expressing GST-Spa40CT, was constructed by inserting a 411 bp *Bam*HI–*Sal*I PCR DNA fragment (obtained using primers Spa40–15 and Spa40–16) into the corresponding sites of pGEX4T1. In pAB51, the GST was inserted in-frame with the last 137 C-terminus residues of Spa40.

Proteins preparation and analysis

Crude extracts and concentrated culture supernatants of *S. flexneri* strains were prepared as described (Allaoui *et al*., 1993; Magdalena *et al*., 2002) and analysed by SDS-PAGE stained with Coomassie blue or Western blot. Briefly, overnight cultures at 37°C were diluted to an OD_{600} of 0.02 in 10 ml TSB and grown at 37°C to an OD_{600} of 2. The culture supernatant was discarded by centrifugation (10 000 *g* for 10 min) and bacterial pellets were re-suspended in 500 μl of PBS containing 100 μg of Congo red (Serva) and incubated at 37°C for 15 min to induce Ipa proteins secretion. Immunodetections were carried out using monoclonal antibodies anti-IpaB (Barzu *et al*., 1993), anti-IpaC (Phalipon *et al*., 1992), and anti-His (Sigma) and polyclonal antibodies anti-Spa32 (Magdalena *et al*., 2002), anti-IpaD (Menard *et al*., 1993) and anti-GST (Amersham).

GST pull-down assay

The GST-Spa40CT derivatives bound to gluthathione sepharose 4B (50 μl) were mixed with cleared extract of Δ*spa32* strain harbouring pMJ8 (expressing His-Spa32) or with ammonium sulphate precipitated culture supernatant proteins prepared from wild-type *S. flexneri* and incubated overnight at 4°C. Supernatants were removed by centrifugation and beads were washed with bead-binding buffer (1% Triton X-100 in Tris-buffered saline, pH 7.4) four times. After the final wash, elution was performed with 40 μl of glutathione and 10 μl of SDS-PAGE sample buffer was added to each sample. Bound proteins were analysed by immunoblotting using anti-His Mab, and polyclonal antibodies against Spa32 and IpaD (Ménard *et al*., 1993; Magdalena *et al*., 2002).

Invasion assay

The gentamicin protection assay to assess bacterial invasion in HeLa cells was described previously (Sansonetti *et al*., 1986). Briefly, 2 ml of wild-type *Shigella* or Δ*spa32* mutant (Magdalena *et al*., 2002) either alone or complemented with plasmids producing His-Spa32, wild-type or variants, was grown to exponential growth phase (OD_{600} = 0.4) and centrifuged onto plates containing 2×10^5 Hela cells at 2000 *g* for 10 min. After 1 h incubation at 37°C, cells were washed three times with 2 ml EBSS and incubated during 1 h with the 2 ml MEM milieu containing gentamicin at 50 μg ml^{-1} final concentration. After three washes with 2 ml EBSS, plates were incubated for 15 min with a solution of desoxycholate 0.5% to allow cells lysis. Bacterial solutions were then diluted and plated on agar plates containing selective antibiotics for colony-forming unit counting.

Electron microscopy analysis

The various strains expressing different *spa32* deletion genes were grown overnight in TSB supplemented with kana-

mycin (50 μg ml^{-1}) at 30°C to an optical density (OD) of 1.3 at 600 nm. The strains were diluted to OD_{600} of 0.1 and grown for a further 4 h at 37°C. Cultured cells were harvested at 2000 *g* and re-suspended in 50 mM phosphate buffer (pH 7.0). Bacteria samples were applied to freshly glow-discharged carbon-coated grids and negatively stained with 2% (w/v) uranylacetate. Visualization of the cells was performed on a Philips CM120FEG operating at 120 kV. Images were recorded with a Gatan 4000 SP 4K slow-scan CCD camera at various magnifications. Needle sizes were measured with the 'Groningen Image Processing' software packages (W. Keegstra, unpublished).

Acknowledgements

This study was supported in part by grants from the Belgian FRSM (Fonds National de la Recherche Scientifique Médicale, Convention: 3.4623. 06). A.B. was supported by a fellowship from Fonds National de la Recherche Industrielle et Agronomique (Belgium). Part of this work was supported by grants from the Fonds of Emile Defay (ULB) and from the Alice and David Van Buuren foundation (ULB). We thank A. Marty for critical reading of this manuscript and R. Dagci for technical assistance.

References

Agrain, C., Callebaut, I., Journet, L., Sorg, I., Paroz, C., Mota, L.J., and Cornelis, G.R. (2005) Characterization of a Type III secretion substrate specificity switch (T3S4) domain in YscP from *Yersinia enterocolitica*. *Mol Microbiol* **56:** 54–67.

Allaoui, A., Sansonetti, P.J., and Parsot, C. (1992) MxiJ, a lipoprotein involved in secretion of *Shigella* Ipa invasins, is homologous to YscJ, a secretion factor of the *Yersinia* Yop proteins. *J Bacteriol* **174:** 7661–7669.

Allaoui, A., Menard, R., Sansonetti, P.J., and Parsot, C. (1993) Characterization of the *Shigella flexneri ipgD* and *ipgF* genes, which are located in the proximal part of the *mxi* locus. *Infect Immun* **61:** 1707–1714.

Barzu, S., Nato, F., Rouyre, S., Mazie, J.C., Sansonetti, P., and Phalipon, A. (1993) Characterization of B-cell epitopes on IpaB, an invasion-associated antigen of *Shigella flexneri*: identification of an immunodominant domain recognized during natural infection. *Infect Immun* **61:** 3825–3831.

Blocker, A., Gounon, P., Larquet, E., Niebuhr, K., Cabiaux, V., Parsot, C., and Sansonetti, P. (1999) The tripartite type III secreton of *Shigella flexneri* inserts IpaB and IpaC into host membranes. *J Cell Biol* **147:** 683–693.

Blocker, A., Jouihri, N., Larquet, E., Gounon, P., Ebel, F., Parsot, C., *et al.* (2001) Structure and composition of the *Shigella flexneri* 'needle complex', a part of its type III secreton. *Mol Microbiol* **39:** 652–663.

Cornelis, G.R. (2006) The type III secretion injectisome. *Nat Rev Microbiol* **4:** 811–825.

Deane, J.E., Graham, S.C., Mitchell, E.P., Flot, D., Johnson, S., and Lea, S.M. (2008) Crystal structure of Spa40, the specificity switch for the *Shigella flexneri* type III secretion system. *Mol Microbiol* **69:** 267–276.

Edqvist, P.J., Olsson, J., Lavander, M., Sundberg, L., Forsberg, A., Wolf-Watz, H., and Lloyd, S.A. (2003) YscP and YscU regulate substrate specificity of the *Yersinia* type III secretion system. *J Bacteriol* **185:** 2259–2266.

Espina, M., Olive, A.J., Kenjale, R., Moore, D.S., Ausar, S.F., Kaminski, R.W., *et al.* (2006) IpaD localizes to the tip of the type III secretion system needle of *Shigella flexneri*. *Infect Immun* **74:** 4391–4400.

Galan, J.E., and Wolf-Watz, H. (2006) Protein delivery into eukaryotic cells by type III secretion machines. *Nature* **444:** 567–573.

Hale, T.L. (1991) Genetic basis of virulence in *Shigella* species. *Microbiol Rev* **55:** 206–224.

Hirano, T., Yamaguchi, S., Oosawa, K., and Aizawa, S. (1994) Roles of FliK and FlhB in determination of flagellar hook length in *Salmonella typhimurium*. *J Bacteriol* **176:** 5439–5449.

Hueck, C.J. (1998) Type III protein secretion systems in bacterial pathogens of animals and plants. *Microbiol Mol Biol Rev* **62:** 379–433.

Journet, L., Agrain, C., Broz, P., and Cornelis, G.R. (2003) The needle length of bacterial injectisomes is determined by a molecular ruler. *Science* **302:** 1757–1760.

Kimbrough, T.G., and Miller, S.I. (2000) Contribution of *Salmonella typhimurium* type III secretion components to needle complex formation. *Proc Natl Acad Sci USA* **97:** 11008–11013.

Kubori, T., Matsushima, Y., Nakamura, D., Uralil, J., Lara-Tejero, M., Sukhan, A., *et al.* (1998) Supramolecular structure of the *Salmonella typhimurium* type III protein secretion system. *Science* **280:** 602–605.

Kubori, T., Sukhan, A., Aizawa, S.I., and Galan, J.E. (2000) Molecular characterization and assembly of the needle complex of the *Salmonella typhimurium* type III protein secretion system. *Proc Natl Acad Sci USA* **97:** 10225–10230.

Magdalena, J., Hachani, A., Chamekh, M., Jouihri, N., Gounon, P., Blocker, A., and Allaoui, A. (2002) Spa32 regulates a switch in substrate specificity of the type III secreton of *Shigella flexneri* from needle components to Ipa proteins. *J Bacteriol* **184:** 3433–3441.

Makishima, S., Komoriya, K., Yamaguchi, S., and Aizawa, S.I. (2001) Length of the flagellar hook and the capacity of the type III export apparatus. *Science* **291:** 2411–2413.

Marlovits, T.C., Kubori, T., Lara-Tejero, M., Thomas, D., Unger, V.M., and Galán, J.E. (2006) Assembly of the inner rod determines needle length in the type III secretion injectisome. *Nature* **441:** 637–640.

Menard, R., Sansonetti, P.J., and Parsot, C. (1993) Nonpolar mutagenesis of the *ipa* genes defines IpaB, IpaC, and IpaD as effectors of *Shigella flexneri* entry into epithelial cells. *J Bacteriol* **175:** 5899–5906.

Minamino, T., and Macnab, R.M. (2000) Domain structure of *Salmonella* FlhB, a flagellar export component responsible for substrate specificity switching. *J Bacteriol* **182:** 4906–4914.

Minamino, T., and Pugsley, A.P. (2005) Measure for measure in the control of type III secretion hook and needle length. *Mol Microbiol* **56:** 303–308.

Minamino, T., Saijo-Hamano, Y., Furukawa, Y., Gonzalez-Pedrajo, B., Macnab, R.M., and Namba, K. (2004) Domain

organization and function of *Salmonella* FliK, a flagellar hook-length control protein. *J Mol Biol* **341:** 491–502.
Minamino, T., Ferris, H.U., Moriya, N., Kihara, M., and Namba, K. (2006) Two parts of the T3S4 domain of the hook-length control protein FliK are essential for the substrate specificity switching of the flagellar type III export apparatus. *J Mol Biol* **362:** 1148–1158.
Moriya, N., Minamino, T., Hughes, K.T., Macnab, R.M., and Namba, K. (2006) The type III flagellar export specificity switch is dependent on FliK ruler and a molecular clock. *J Mol Biol* **359:** 466–477.
Mota, L.J., Journet, L., Sorg, I., Agrain, C., and Cornelis, G.R. (2005) Bacterial injectisomes: needle length does matter. *Science* **307:** 1278.
Parsot, C., Ageron, E., Penno, C., Mavris, M., Jamoussi, K., d'Hauteville, H., *et al.* (2005) A secreted anti-activator, OspD1, and its chaperone, Spa15, are involved in the control of transcription by the type III secretion apparatus activity in *Shigella flexneri*. *Mol Microbiol* **56:** 1627–1635.
Phalipon, A., Arondel, J., Nato, F., Rouyre, S., Mazie, J.C., and Sansonetti, P.J. (1992) Identification and characterization of B-cell epitopes of IpaC, an invasion-associated protein of *Shigella flexneri*. *Infect Immun* **60:** 1919–1926.
Sani, M., Botteaux, A., Parsot, C., Sansonetti, P., Boekema, E.J., and Allaoui, A. (2007a) IpaD is localized at the tip of the *Shigella flexneri* type III secretion apparatus. *Biochim Biophys Acta* **1770:** 307–311.
Sani, M., Allaoui, A., Fusetti, F., Oostergetel, G.T., Keegstra, W., and Boekema, E.J. (2007b) Structural organization of the needle complex of the type III secretion apparatus of *Shigella flexneri*. *Micron* **38:** 291–301.
Sansonetti, P.J., Ryter, A., Clerc, P., Maurelli, A.T., and Mounier, J. (1986) Multiplication of *Shigella flexneri* within HeLa cells: lysis of the phagocytic vacuole and plasmid-mediated contact hemolysis. *Infect Immun* **51:** 461–469.
Shibata, S., Takahashi, N., Chevance, F.F., Karlinsey, J.E., Hughes, K.T., and Aizawa, S. (2007) FliK regulates flagellar hook length as an internal ruler. *Mol Microbiol* **64:** 1404–1415.
Tamano, K., Katayama, E., Toyotome, T., and Sasakawa, C. (2002) *Shigella* Spa32 is an essential secretory protein for functional type III secretion machinery and uniformity of its needle length. *J Bacteriol* **184:** 1244–1252.
West, N.P., Sansonetti, P., Mounier, J., Exley, R.M., Parsot, C., Guadagnini, S., *et al.* (2005) Optimization of virulence functions through glucosylation of *Shigella* LPS. *Science* **307:** 1313–1317.
Williams, A.W., Yamaguchi, S., Togashi, F., Aizawa, S.I., Kawagishi, I., and Macnab, R.M. (1996) Mutations in *fliK* and *flhB* affecting flagellar hook and filament assembly in *Salmonella typhimurium*. *J Bacteriol* **178:** 2960–2970.

Supporting information

Additional supporting information may be found in the online version of this article.

Please note: Wiley-Blackwell are not responsible for the content or functionality of any supporting materials supplied by the authors. Any queries (other than missing material) should be directed to the corresponding author for the article.

